Journal of Dental Sciences 19 (2024) 231–245

Available online at www.sciencedirect.com

ScienceDirect

journal homepage: www.e-jds.com

Original Article

Nicotine destructs dental stem cell-based periodontal tissue regeneration

Yuran Jiang [a†], Kuan Yang [b†], Bo Jia [c†], Yuan Gao [c,d], Yujiang Chen [a], Peng Chen [a], Xiaoxi Lu [a], Wei Zhang [c], Xiaojing Wang [a*]

[a] *State Key Laboratory of Military Stomatology, National Clinical Research Center for Oral Diseases, Shaanxi Key Laboratory of Stomatology, School of Stomatology, Fourth Military Medical University, Xi'an, Shaanxi, China*
[b] *School of Stomatology, Qingdao University, Qingdao, Shandong, China*
[c] *State Key Laboratory of Cancer Biology, Biotechnology Center, School of Pharmacy, Forth Military Medical University, Xi'an, Shaanxi, China*
[d] *School of Biomedical Science, Li Ka-shing School of Medicine, Hong Kong University, Hong Kong, China*

Received 5 April 2023; Final revision received 18 April 2023
Available online 3 May 2023

KEYWORDS
Human periodontal ligament stem cells (hPDLSCs);
Smoking;
Periodontitis;
Regeneration;
Bone remodeling/resorption;
Sequence analysis

Abstract *Background/purpose:* Nicotine is a widely known addictive and toxic substance in cigarette that exacerbates periodontitis. However, its deleterious effects on dental stem cells and subsequent implications in tissue regeneration remain unclear. This study aimed to explore the effects of nicotine on the regenerative capacity of human periodontal ligament stem cells (hPDLSCs) based on transcriptomics and proteomics, and determined possible targeted genes associated with smoking-related periodontitis.
Materials and methods: hPDLSCs were treated with different concentrations of nicotine ranging from 10^{-3} to 10^{-8} M. Transcriptomics and proteomics were performed and confirmed employing Western blot, 5-ethynyl-2′-deoxyuridine (EdU), and alkaline phosphatase (ALP) staining. A ligature-induced periodontitis mouse model was established and administrated with nicotine (16.2 μg/10 μL) *via* gingival sulcus. The bone resorption was assessed by micro-computed tomography and histological staining. Key genes were identified using multi-omics analysis with verifications in hPDLSCs and human periodontal tissues.
Results: Based on enrichments analysis, nicotine-treated hPDLSCs exhibited decreased proliferation and differentiation abilities. Local administration of nicotine in mouse model significantly aggravated bone resorption and undermined periodontal tissue regeneration by inhibiting the endogenous dental stem cells regenerative ability. HMGCS1, GPNMB, and CHRNA7 were hub-genes according to the network analysis and corelated with proliferation

* Corresponding author. Department of Pediatric Dentistry, School of Stomatology, Fourth Military Medical University, 145# West Changle Rd, Xi'an, Shaanxi, 710032, China.
E-mail address: 1092487765@qq.com (X. Wang).
† Authors contributing equally to this article.

https://doi.org/10.1016/j.jds.2023.04.018

and differentiation capabilities, which were also verified in both cells and tissues.
Conclusion: Our study investigated the destructive effects of nicotine on the regeneration of periodontal tissues from aspects of in vitro and in vivo with the supporting information from both transcriptome and proteome, providing novel targets into the molecular mechanisms of smoking-related periodontitis.

Introduction

Chronic periodontitis is a common and worldwide disease that irreversibly destructs the complex structures of periodontal tissues comprising the alveolar bone, cementum, and periodontal ligament (PDL), eventually leading to tooth loss.[1,2] Cigarette smoking is the most important risk factor of periodontitis.[3–5] Cigarette smoking also promotes a poor clinical response to the regenerative periodontal procedures.[6] The World Health Organization estimates that the number of smokers worldwide will exceed 1.7 billion by 2025.[7] To date, however, the acute cellular mechanisms by which smoking exacerbates the severity of periodontitis and destructs periodontal tissue regenerative capacity have not been completely elucidated.

Recent advances in stem cell biology and regenerative medicine, aiming to improve the efficacy and predictability of periodontal regenerative therapies, have resulted in novel cell-based therapeutic approaches.[8,9] hPDLSCs have raised many concerns owing to their great potential of tissue regeneration to remodel alveolar bone formation.[10,11] However, hPDLSCs-based therapy for tissue regeneration displays high sensitivity to tissue origin and is vulnerable to external stimulations, including chemical substances and inflammatory factors.[12] The major success of hPDLSCs in clinical regeneration practice relies not only on enhancing cell regeneration capacity but also on investigating susceptibility to exogenous factors to provide supportive suggestions for donor selections.[13] Thus, it is of great importance to consider the impact of destructive factors that inhibit cellular therapeutic regeneration.

Nicotine is one of the major toxic components of cigarettes that leads to addiction and adversely affects cardiovascular, digestive, reproductive, respiratory, and immune systems.[14] As the smoke enters the oral cavity, the nicotine concentration becomes higher in the saliva than in the blood, indicating the crucial role of nicotine in periodontitis.[15] At the cellular level, nicotine can impair the regenerative capacity of mesenchymal stem cell (MSC) populations,[16] which may justify the support for further research on hPDLSCs regeneration.[5]

To the best of our knowledge, the current study is the first to further explore the destructive effects of nicotine on hPDLSC-based periodontal tissue regeneration by integrating the transcriptome and proteome analysis that were validated in both in vivo and in vitro. Our study provides novel insights into the potential therapeutic targets for individualized treatment of smoking-related periodontitis and establish criteria for donor selection of tissue regeneration.

Materials and methods

Study subjects and ethics statement

Human periodontal ligament tissues were obtained from patients undergoing a third molar extraction. The pack-year of eight individuals is over 20 (mean age, 39.8 years) while 10 healthy donors is 0 (mean age, 27.4 years). All volunteers were from the School of Stomatology, Fourth Military Medical University and provided a written informed consent prior to the commencement of the study. The investigation was approved by the Ethics Committee of School of Stomatology, Forth Military Medical University, and was conducted in accordance with the Declaration of Helsinki. Further details of the periodontal status of donors were presented in the Appendix Table 1.

Cell culture and nicotine treatment

hPDLSCs were obtained from healthy and intact permanent teeth undergoing orthodontic extractions from 10 donors aged 20—34 years. The inclusion and exclusion criteria were presented in the Appendix Table 2. hPDLSCs were inoculated into a complete medium containing different concentrations of nicotine solution (Sigma-Aldrich, St. Louis, MO, USA) ranging from 10^{-3} to 10^{-8} M for 48 h. The nicotine solution was diluted in complete medium. More detailed information on cell isolation was presented in the Appendix of materials and methods.

Animal experiments

Eight-week-old C57BL/6 male mice were housed under specific pathogen-free and controlled temperature conditions, and were maintained under 12 h light—dark cycle. All animal experiments were performed according to the guidelines of the Laboratory Animal Care & Welfare Committee, School of Stomatology, Fourth Military Medical University (FMMU; protocol number: 2020004) and Animal Research: Reporting of In Vivo Experiments (ARRIVE). To mimic periodontitis environment, the cervical area of the maxillary second molar was ligated with a sterile silk thread (5—0) under general anesthesia. For the group with nicotine-induced periodontitis, a solution of 10^{-5} M nicotine was injected into the gingival sulcus on days 3, 6, 9,

and 12, while PBS (Gibco, Grand Island, NY, USA) was used in control and ligated groups. Each group included 5 mice. After 14 days, the maxilla was removed and fixed in 4% paraformaldehyde (NCM Biotech, Suzhou, China) for further analysis.

Transcriptomic profiling

hPDLSCs in the control group (cultured in normal complete medium, n = 3) and nicotine group (cultured in complete medium containing 10^{-5} M nicotine, n = 3) were harvested after reaching 80% confluence. For each transcription region, a fragment per kilobase of transcript per million mapped reads (FPKM) value was calculated to quantify its expression abundance and variations, using the StringTie software. The detailed information and RNA sequencing analysis were presented in the Appendix of materials and methods.

Proteomic profiling

Tandem mass tagging labeling and liquid chromatography tandem mass spectrometry analysis were performed. Proteins were classified by GO annotation into three categories: biological process, cellular compartment, and molecular function. The detailed information was presented in the Appendix of materials and methods.

Statistical analysis

Statistical analysis was conducted using Prism 9 (GraphPad Software Inc). Data were presented as the mean ± standard deviation (SD). Statistically significant differences between two groups were analyzed using an independent unpaired two-tailed Student's *t*-tests and were indicated in the figures as follows: ns $P > 0.05$, $^{*}P < 0.05$, $^{**}P < 0.01$, $^{***}P < 0.001$, and $^{****}P < 0.0001$.

The detailed information of the following methods was presented in the Appendix of materials and methods: Cell migration; CCK-8 assay; Real-time cellular analysis (RTCA); Colony-forming assay; 5-ethynyl-2′-deoxyuridine (EdU) staining assay; ALP staining and Alizarin Red Staining; ALP activity assay; Micro-computed tomography (Micro-CT); Histological staining (HE, MASSON, TRAP); Immunohistochemistry; RNA extraction and Quantitative Real-Time Polymerase Chain Reaction (qRT-PCR); Western Blot (WB) and immunofluorescence (IF); Enzyme-linked immunosorbent assay (ELISA); and Flow Cytometric Analysis.

Results

Nicotine alters hPDLSCs characteristics

The effect of nicotine on the morphology, viability, and motility of hPDLSCs was observed in the presence of different concentrations of nicotine (Fig. 1a). hPDLSCs were identified positively expressed MSC markers CD73, CD90, CD105 while negatively for CD34, CD45, and CD14 by flow cytometric detection (Fig. 1b). The morphology of hPDLSCs in 10^{-3}, 10^{-4}, and 10^{-5} M nicotine-treated groups exhibited partially round-shaped and vacuolated morphology (Fig. 1c). We noted a great reduction in the hPDLSCs migration distance in cells treated with 10^{-3} and 10^{-4} M concentrations, whereas no significant difference was observed in the 10^{-7} and 10^{-8} M nicotine-treated groups versus control group (Fig. 1d and e). According to CCK-8 assay, the viability of hPDLSCs cultured in the presence of 10^{-5} M nicotine was significantly inhibited. Interestingly, hPDLSC growth surged in 10^{-3} and 10^{-4} M nicotine-treated groups within the first 20 h, after which the growth curve declined rapidly, indicating that persistent stimulation by high concentrations of nicotine was lethal to hPDLSCs (Fig. 1f).

Nicotine promotes the release of inflammatory factors of hPDLSCs

The 10^{-5} M nicotine concentration exerted maximum inhibition of hPDLSCs with minor cell death and was selected for the following assay. The induction of nicotine obviously reduced the stemness of hPDLSCs by downregulated the expression of CD105 and CD 90 (Fig. 1g). In addition, nicotine treatment increased both mRNA and protein expression levels of inflammatory factors including IL-1β, TNF-α, and IL-6 in hPDLSCs (Fig. 1h and i). Taken together, nicotine inhibited the viability and motility of hPDLSCs and increased the levels of IL-1β, TNF-α, and IL-6, which partially simulated the periodontitis micro-environment in vitro.

Transcriptomic and proteomic analysis reveal functional alterations in nicotine-treated hPDLSCs

To further explore nicotine-induced alterations in the biological function of hPDLSCs, we performed both transcriptome and proteome profiling of the control- and nicotine-treated groups (Fig. 2a). For transcriptomics, a total of 3263 hPDLSC genes significantly changed their expression levels; fold change (FC) level was increased or decreased 1.5 times with $P < 0.05$, including 1608 (49.28%) upregulated and 1655 (50.72%) downregulated genes upon treatment with nicotine (Fig. 2b, Appendix Fig. 1). Notably, the functions associated with cell proliferation, including cell cycle, DNA replication, and chromosome segregation, were included in the top 20 enriched functions according to GO analysis (Fig. 2c). Furthermore, the classification of the top 20 pathways in the Kyoto Encyclopedia of Genes and Genomes (KEGG) analysis also highly focused on cell proliferation-related pathways, such as cell cycle, P53 signaling pathway, and DNA replication (Fig. 2d). We further performed a gene set enrichment analysis (GSEA), which supplements and identifies the functions of the prior gene sets for GO analysis,[37,38] to indicate that osteoclast and osteoblast differentiation combined with bone regulation were highly enriched (Fig. 2e).

Using quantitative label-free mass spectrometry, we detected 136 differently ex-pressed proteins in nicotine-treated cells in triplicates, with the condition of increased or decreased 1.2 times FC level and $P < 0.05$. Among these, 86 proteins (63.24%) were up-regulated, while 50 (36.76%) were down-regulated (Fig. 2f, Appendix Fig. 1). The

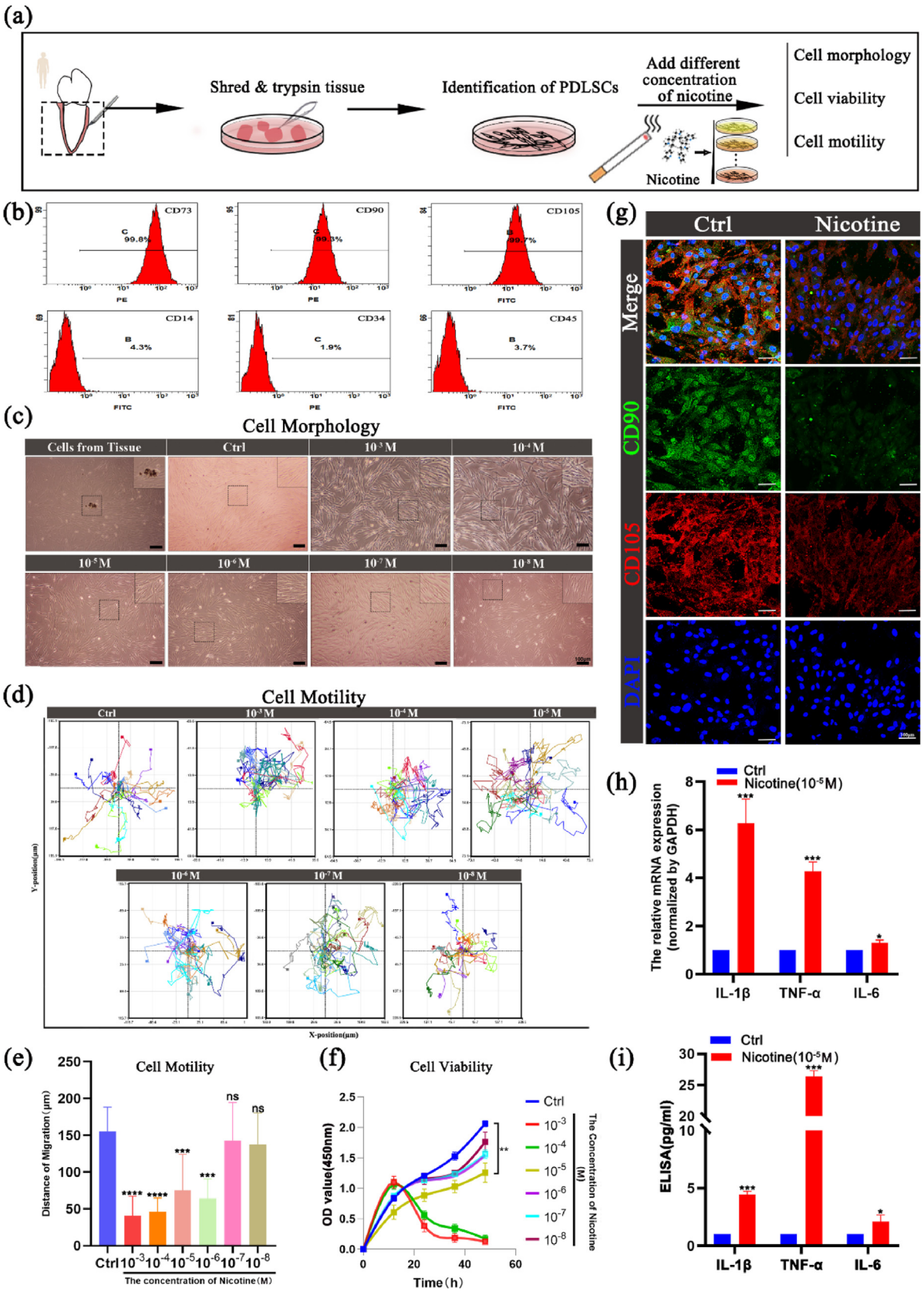

Figure 1 Nicotine with different concentrations inhibit viability and motility of hPDLSCs while promote the release of inflammatory factors. (a) Immunophenotyping of PDLSCs with flow cytometric analysis. PDLSCs positively expressed stem cell markers CD73, CD90, and CD105 while negatively expressed CD14, CD34, and CD45. (b) IF staining images for mesenchymal stem cell markers. hPDLSCs positively expressed CD73 (green) and Stro-1 (red). The nuclei were stained by DAPI (blue). (c) Representative

classification of GO enrichment analysis was enriched in the functions of cell motility and cell proliferation (Fig. 2g, Appendix Fig. 1). In addition, differentiation-related pathways, such as osteoclast differentiation and JAK-STAT signaling pathway were also highly enriched (Fig. 2h). Collectively, these findings suggested that nicotine possibly effected the regeneration (proliferation and osteoblastogenesis/osteoclastogenesis differentiation) capacity of hPDLSCs.

Nicotine inhibits hPDLSCs proliferation ability in vitro

Next, we evaluated the effect of nicotine on proliferation of hPDLSCs in vitro. The GSEA further confirmed that the stem cell proliferation was highly enriched upon nicotine treatment (Fig. 3a). Subsequently, colony-forming assay results showed that nicotine significantly reduced the number of colonies (Fig. 3b). Besides, the RTCA also revealed that nicotine treatment reduced the viability of hPDLSCs (Fig. 3c). In addition, nicotine largely reduced the percentage of proliferation marker $Ki67^+$ in hPDLSCs versus the control group (Fig. 3d). Meanwhile, both mRNA and protein expression of proliferating cell nuclear antigen (PCNA) were greatly reduced upon treatment with nicotine (Fig. 3f). EdU staining of the nuclei in nicotine-treated hPDLSCs was significantly decreased, indicating retardation of DNA replication (Fig. 3e). Thereafter, we measured the molecular regulation of cell cycle after nicotine treatment by conducting a quantitative Real-Time Polymerase Chain Reaction (qRT-PCR) and Western Blot (WB). The results showed that P53 and P16, both of which are well-known inhibitors of cell cycle progression and control the cellular senescence simultaneously, levels were elevated by nicotine treatment (Fig. 3g and h). Besides, flow cytometry analysis revealed a significant decrease of the G2/M phase rate while an increase of Annexin V^+ apoptosis for nicotine-treated hPDLSCs (Fig. 3i and j). These results suggested that nicotine inhibited the proliferation of hPDLSCs through re-pressing DNA replication and cell cycle arresting.

Nicotine disturbs the balance of osteoblastogenesis/osteoclastogenesis differentiation for hPDLSCs in vitro

Nicotine-treated hPDLSCs exhibited poor osteogenic ability, as indicated by the suppressed alkaline phosphatase (ALP) activity and decreased mineralized nodule formation (Fig. 4a–d). Parallel studies also revealed reduced expression levels of ALP, osteocalcin (OCN), runt-related transcription factor 2 (RUNX2), and bone integrin-binding sialoprotein (BSP), as confirmed by the qRT-PCR and WB analyses (Fig. 4e, g). In contrast, the mRNA and protein expression levels of receptor activator of nuclear factor-kappa B ligand (RNAKL) were significantly increased, while that of the osteoclastogenesis inhibitory factor, osteoprotegerin (OPG), was largely decreased (Fig. 4f and g). These results indicated that nicotine disturbed the balance of hPDLSC differentiation by increasing their osteoclastogenesis while simultaneously decreasing their osteoblastogenesis potential.

Nicotine exacerbates periodontitis phenotypes in mice

Based on our results that nicotine could release inflammatory factors of hPDLSCs, we then investigated whether nicotine could exacerbate bone resorption in vivo. Therefore, we established a ligature-induced periodontitis mouse model with an activated pro-inflammatory micro-environment.[36] Local administration of PBS/nicotine was conducted separately on days 3, 6, 9, and 12 after ligation (Fig. 5a). Micro-CT revealed severe alveolar bone resorption in the periodontitis group compared to the control group, indicating successful establishment of periodontitis (white dotted area, Fig. 5b). Subsequently, nicotine treatment increased the distance from cementoenamel junction to alveolar bone crest (Fig. 5c). The nicotine group also showed a greater bone resorption compared to ligated and control groups as measured by bone volume/total volume (BV/TV), trabecular separation (Tb.Sp), trabecular number (Tb.N), trabecular bone pattern factor (Tb.Pf), and trabecular thickness (Tb.Th) (Fig. 5g–k). Furthermore, nicotine-treated mice displayed a greater degree of local inflammation than the ligation group, including elevated inflammatory cell infiltration, hydrolytic and necrotic tissue, and crypt damage, which resulted in deeper periodontal pockets localized not only between the root and alveolar crest, but also in the root furcation (Appendix Fig. 2). The immunohistochemistry (IHC) results also showed that the ex-pression of inflammatory factors (IL-1β, TNF-α, and IL-6) increased in the nicotine group compared to the control group (Fig. 5f, Appendix Fig. 2), which was consistent with the in vitro results. To investigate nicotine-induced soft tissue damage, Masson staining results demonstrated fragmentation, denaturation, and partially vacuolated degeneration of periodontal collagen fibers (Fig. 5d, Appendix Fig. 2). Furthermore, TRAP assay revealed the presence of more $Trap^+$ cells in the nicotine-treated group compared to the ligation counterpart (Fig. 5e, Appendix Fig. 2).

Nicotine influences the regeneration capability of endogenous dental stem cells in vivo

The influence of nicotine on the regeneration ability of endogenous dental stem cells localized in periodontal

image of hPDLSCs morphology with different nicotine concentrations. The (d, e) motility and (f) viability of hPDLSCs in control, 10^{-3}, 10^{-4}, 10^{-5}, 10^{-6}, 10^{-7}, and 10^{-8} M nicotine groups in vitro. (g) Representative image of IF staining for control and nicotine-treated hPDLSCs: CD90 (green), CD105 (red), and DAPI (blue), which were significantly decreased in nicotine group verses control group. (h) The effects of nicotine treatment on the release of inflammatory cytokines for 48 h in hPDLSCs by qRT-PCR. GAPDH was used for normalization relative to the control group. (i) EILSA analyses showed the protein expression level of inflammatory cytokines induced by nicotine in hPDLSCs. Mean ± SD. ns $P < 0.05$. *$P < 0.05$. **$P < 0.01$. ***$P < 0.001$. ****$P < 0.0001$.

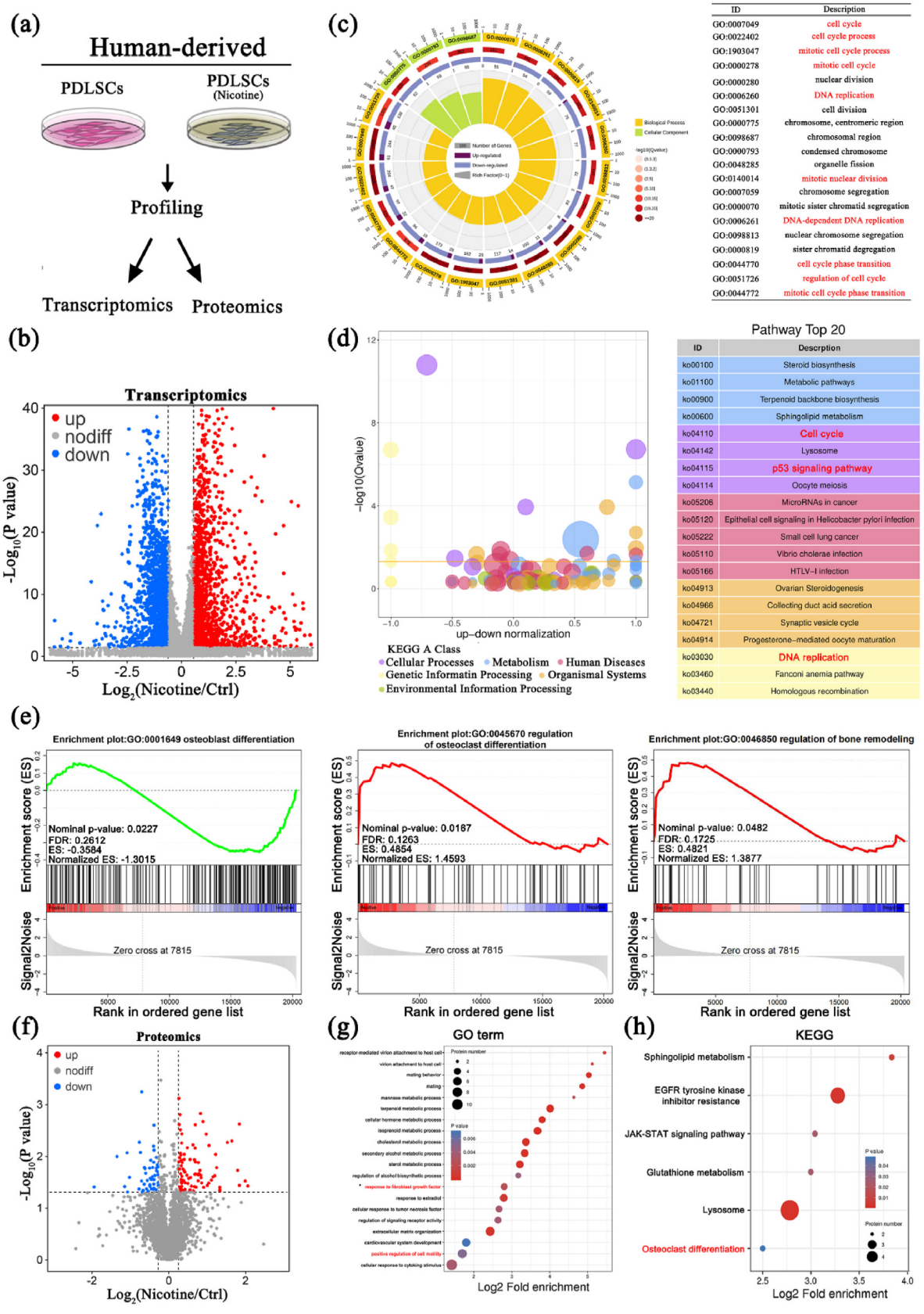

Figure 2 Transcriptomic and proteomic analysis of hPDLSCs treated by nicotine. (a) We used human-derived PDLSCs with/without nicotine treatment to perform transcriptomics and proteomics, respectively. (b–e) RNA-sequencing analysis. (b) Volcano map and histogram of different expressed genes in mRNA level between control and nicotine-treated groups. Red dots represent up-regulated genes and blue dots represent down-regulated genes. (c) The circle diagram represents gene ontology (GO)

ligament in vivo was evaluated employing IF. The results showed that the expression of RANKL increased while RUNX2 obviously decreased in the nicotine group (Fig. 6a–c). In order to localize and investigate the proliferation ability of endogenous dental stem cells in periodontal ligament tissues, we stained both MSC marker Sac-1 and proliferation marker Ki67 for IF. The results suggested that Sac-1^{+} and Ki67^{+} cells were both decreased in the nicotine group (Fig. 6d–f).

Collectively, these data confirmed that nicotine could aggravate the phenotypes of periodontitis in vivo and destructs the periodontal tissue regeneration by inhibiting endogenous dental stem cells proliferation and differentiation abilities.

Correlation of HMGCS1, GPNMB, and CHRNA7 genes with proliferation and differentiation in nicotine-treated hPDLSCs

Because of the discrepancies between mRNA and protein expressions, we per-formed a multi-omics analysis of transcriptome and proteome to filter key genes with consistent variation trends. A total of 4033 genes quantified co-expressed in RNA-seq and proteomic profiling (Appendix Fig. 3). Subsequently, we used a nine-quadrant volcano map to classify these genes according to different expression levels of mRNA and proteins (Fig. 7a). The most notable quadrants included genes with consistent mRNA and protein expression, suggesting that the post-translational modification was unregulated or less regulated, which belonged to quadrant 3 (84 genes) and quadrant 7 (91 genes). These data prompted us to further investigate whether genes located in these two quadrants were enriched in proliferation and differentiation functions. GO enrichment analysis revealed 14 differentiation- and 17 proliferation-related genes in quadrants 3 and 7, respectively (Appendix Fig. 3). To further explore the key genes, we then mapped the protein-protein interaction (PPI) networks using the Cytoscape software to detect hub genes of these two functions, suggesting that HMGCS1 and GPNMB were the dominant proliferation- and differentiation-related genes, respectively, by applying the cytoHubba plug-in calculated with Maximal Clique Centrality (MCC; Fig. 7b). We then performed correlation analysis of the top 20 genes, according to their expression levels, which showed that the CHRNA7 was correlated with both proliferation and differentiation functions and was selected as the third key gene (Fig. 7c). The FPKM values for HMGCS1, GPNMB, and CHRNA7 were up-regulated after nicotine treatment (Fig. 7d). Overall, HMGCS1, GPNMB, and CHRNA7 were the key genes associated with proliferation and differentiation of nicotine-treated hPDLSCs.

Expression validation of key genes in hPDLSCs and human periodontal ligament tissues

Specifically, we performed qRT-PCR and WB to verify the in vitro expression of HMGCS1, GPNMB, and CHRNA7. The results showed that both mRNA and protein expression levels of three key genes were obviously increased after treatment of nicotine in hPDLSCs (Fig. 8a–c). Besides, we further performed IF staining of Stro-1 with three key genes separately, which showed that the gray values of HMGCS1, GPNMB, and CHRNA7 were increased while Stro-1 was decreased in hPDLSCs after treated by nicotine (Fig. 8d and e). Subsequently, we collected human periodontal ligament tissues from smoking and non-smoking patients to validate the expression of the three key genes influenced by smoking. We observed that the mRNA expressions of HMGCS1, GPNMB, and CHRNA7 were significantly increased in smoking-related periodontal ligament tissues (Fig. 8f). According to HE staining, we found a more sever inflammation infiltration in smoking-related periodontal tissues (Fig. 8g). Besides, results from the representative IHC images also presented more positive areas of HMGCS1, GPNMB, and CHRNA7 in smoking-related periodontal ligament tissues compared with the tissues from non-smokers (Fig. 8h and i). Collectively, we validated that both mRNA and protein expression levels of HMGCS1, GPNMB, and CHRNA7 were obviously in-creased after nicotine treatment in hPDLSCs and smoking-related periodontal tissues, which was in line with the results of sequencing analysis.

Discussion

In this study, we uncovered the destructive effects of nicotine on hPDLSC-based periodontal tissue regeneration from novel insights. Nicotine significantly undermines the regeneration of hPDLSCs by inhibiting the cells proliferation capacity and disturbing the balance of osteoblastogenesis/osteoclastogenesis. Administration of nicotine in mouse models prompted bone resorption and retarded the progression of tissue self-repair by inhibiting the regeneration capacity of dental stem cells in periodontal ligament. A multi-omics analysis identified three promising nicotine-regulated genes which were also validated in hPDLSCs and different human tissues.

It is well established that cigarette smoke is a major risk factor for chronic periodontitis, which is associated with

enrichment analysis. The first circle represents enrichment of top 20 GO terms, outside the circle is the ruler of gene number. Different colors represent different ontologies. The second circle represents the number of GO terms and Q value. The third circle represents up/down-regulated gene ratio bar charts, dark purple represents up-regulated gene ratio, light purple represents down-regulated gene ratio. The fourth circle represents the Rich Factor value of each GO term (the number of differential genes in the GO term divided by all the numbers). The diagram on the right represents the names of top 20 GO terms. (d) The bubble diagram of top 20 kyoto encyclopedia of genes and genomes (KEGG) enrichments. The yellow line in the diagram represents the threshold Q value = 0.05. The diagram on the right represents the names of top 20 KEGG terms. (e) Gene set enrichment analysis (GSEA) of osteoblastogenesis/osteoclastogenesis differentiation and bone remolding for hPDSLCS. Proteomic analysis of (f) Volcano map and histogram, (g) GO analysis, and (h) KEGG analysis.

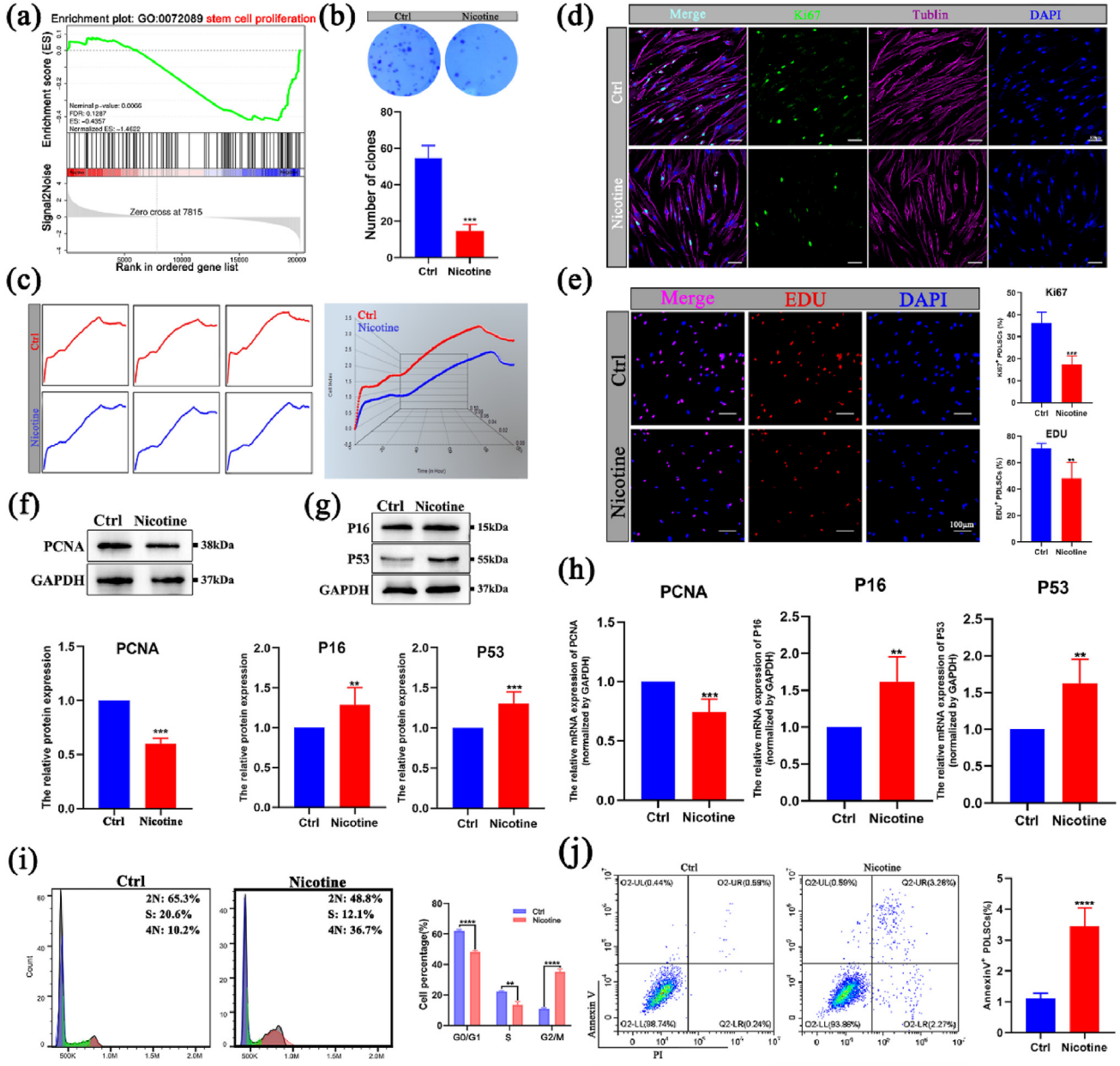

Figure 3 Nicotine obviously inhibits the proliferation capability of hPDLSCs. (a) Representative GSEA diagram of nicotine treatment reduced the function of stem cell proliferation for hPDLSCs. (b) Single-cell forming colony assay shows that less cell colonies were formed in nicotine-treated group versus control group. (c) Real-Time cellular analysis reveals the growth curve of hPDLSCs in control group which is steeper than nicotine-treated group. (d) Representative IF staining of Ki67 (green) and tubulin (purple). (e) Representative IF staining of 5-Ethynyl-2′- deoxyuridine (EdU) assay, nicotine group shows less DNA replication (red) versus control group. Nuclei are stained by DAPI (blue). (f—h) The relative mRNA and protein expression level of PCNA, P16 and P53 with or without nicotine treatment performed by qRT-PCR and WB. GAPDH was used for normalization relative to the control group. Assessment of (i) cell cycle and (j) cell apoptosis with flow cytometric analysis for hPDLSCs with or without nicotine treatment. Mean ± SD. *$P < 0.05$. **$P < 0.01$. ***$P < 0.001$.

inflammatory factors infiltration, alveolar bone resorption, and pocket formation.[17,18] As the major addictive component and predominant toxin found in tobacco leaves, nicotine occupies approximately 95% of the total alkaloids.[19] Previous studies showed that nicotine together with lipopolysaccharide (LPS) stimulates the release of TNF-α, IL-6, IL-12, IL-1β, and matrix metalloproteinases (MMPs).[20—22] In combination with *Escherichia coli* and *Porphyromonas gingivalis*, the nicotine treatment caused an obvious increase of IL-1β and IL-8.[23] These findings suggest that nicotine and bacterial factors interact to affect the host response, but are limited to indicate the effect that nicotine exerts by itself. In our study, we focused on the direct effect of nicotine alone on hPDLSCs and showed that

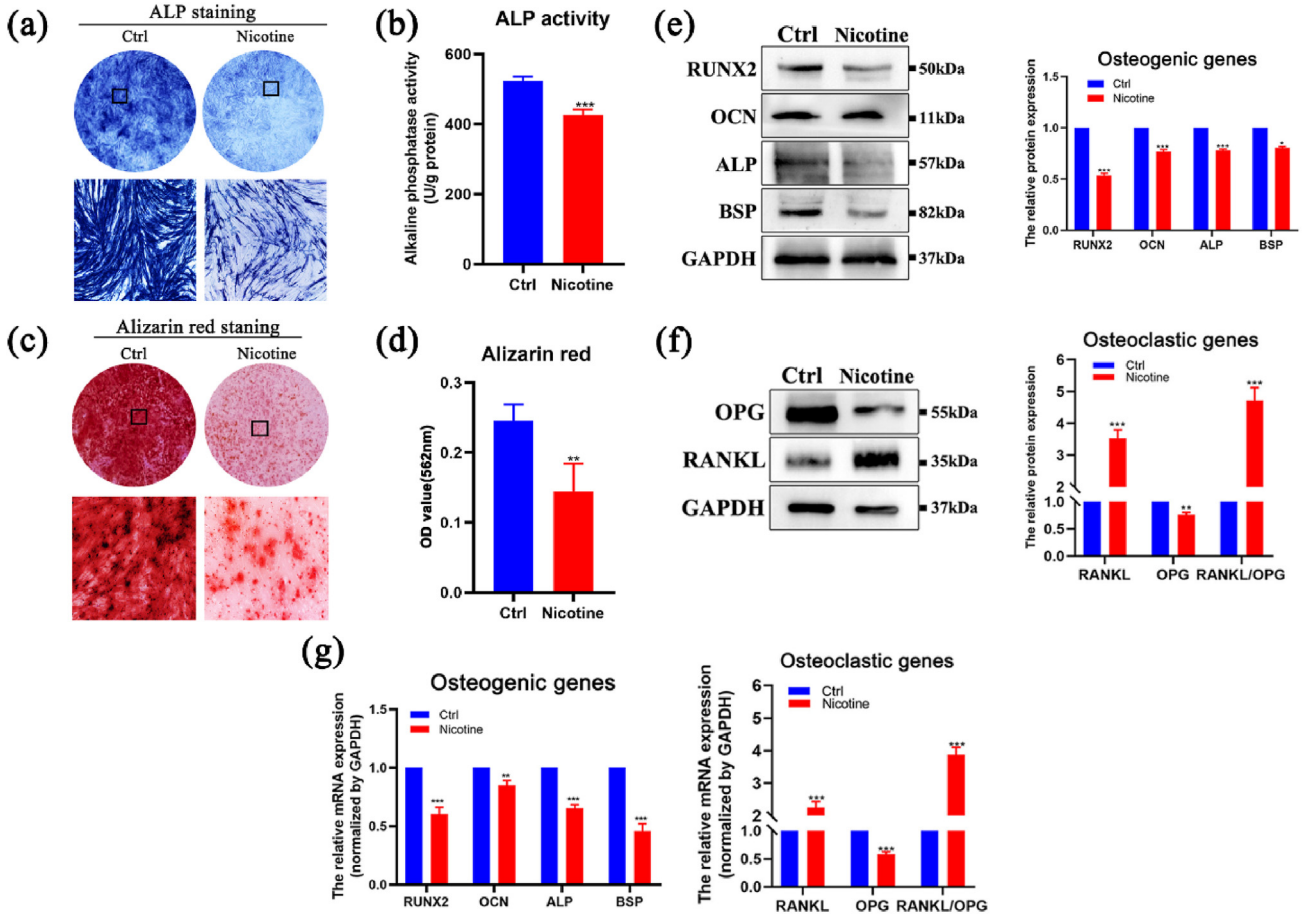

Figure 4 Nicotine disturbs the balance of osteoclastogenesis/osteoblastogenesis differentiation capability of hPDLSCs. (a, b) ALP staining and activity assay. (c, d) Representative images of Alizarin red staining and histogram analysis for mineralized nodules quantification. (e, f) WB analysis for the protein expression level of RUNX2, OCN, ALP, BSP, OPG, and RANK. GAPDH was used to control protein loading. (g) qRT-PCR for mRNA expression level of RUNX2, OCN, ALP, BSP, OPG, and RANKL. GAPDH was used for normalization relative to the control group. Mean ± SD. *$P < 0.05$. **$P < 0.01$. ***$P < 0.001$.

it promotes the release of inflammatory factors IL-1β, TNF-α, and IL-6.

In recent studies, the impact of nicotine on self-renewal and proliferation potential of cells remains controversial, with some reporting a significant decrease in the proliferation and differentiation of nicotine-treated MSCs,[16] while others reporting the promotion of tumor growth and metastasis through an improvement in the self-renewal of nicotine-exposed cells in lung cancer[24] and esophageal cancer.[25] This suggests that nicotine exerts different regulatory effects in different tissues and cell linages. Our data revealed that nicotine exerts anti-proliferative effect because of p53-dependent cell cycle arrest in the G2/M phase mediated by p16 in hPDLSCs, indicating that nicotine dramatically induces an increase in the ratio of cells in the G2/M phase and inhibited the cell division, which lead to the decrease of G0/G1 cells ratio, a quiescent phase of the cell cycle.[26] Interestingly, except for the regulation of cell cycle, it is widely known that p53 and p16 are also typical markers of cellular senescence. Hence, the upregulation of p53 and p16 by induction of nicotine may also suggest that nicotine could influence the pre-senescence of hPDLSCs, which still needs further investigation. Besides, some research revealed that cigarette smoke exposure inhibits osteoclastic apoptosis by increasing the number of osteoclasts through the mtROS/cytochrome C/caspase 3 signaling pathway.[27] In the present study, the results from transcriptome and proteome indicate that nicotine regulates bone remodeling process, as confirmed by the decreased expression of RUNX2, OCN, ALP, BSP, and OPG and increased expression of RANKL in hPDLSCs. Our results were further validated by periodontitis mouse model to show that nicotine exacerbates periodontitis by aggravating inflammatory response and alveolar bone resorption through regulating the re-generation of endogenous stem cells. However, contrary to our findings, Zhou et al. found that nicotine (10^{-9} M) alone did not affect the differentiation ability of hPDLSCs, unless combined with inflammatory factors (IL-1β, TNF-α).[28] This might because the low concentrations of nicotine may be insufficient to induce phenotypic alteration in hPDLSCs.[16] Collectively, our results suggest that nicotine undermines hPDLSCs proliferation and differentiation capacity, which provides information for stem cell-based therapeutic applications.

The analysis of transcriptomics to examine stem cell transcriptional levels is a promising means of identifying

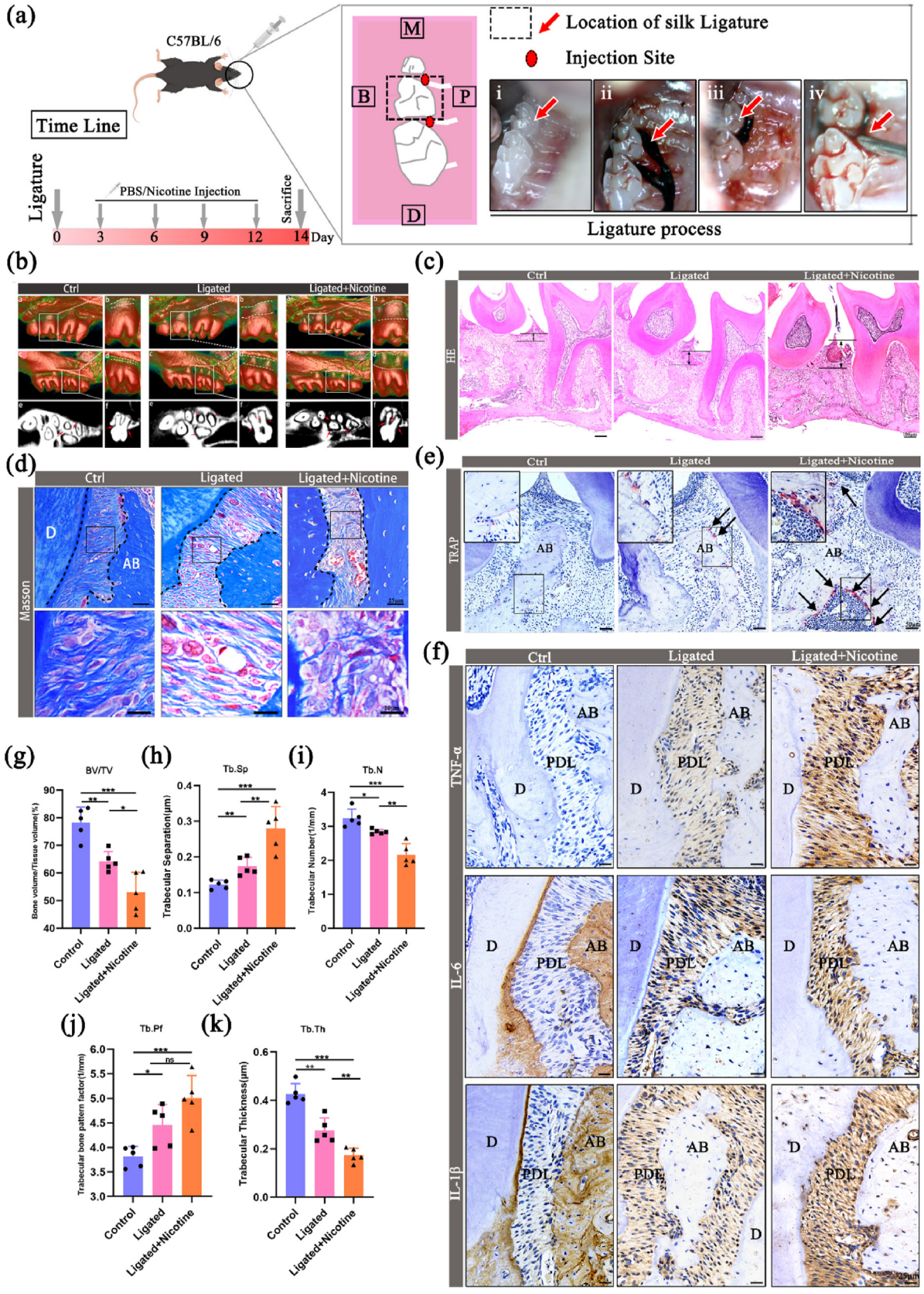

Figure 5 Nicotine exacerbates periodontitis phenotypes in mouse models. (a) Schematic diagram and time line for mouse periodontitis experiment. (b) Representative 3D reconstructed digitized images, including palatal side images, buccal side images, cross section images, and coronal plane images of maxillary second molars analyzed by Micro-CT. Red arrows represents bone resorption areas. (c) Representative hematoxylin and eosin (HE) staining images to analyze periodontal bone resorption, which was

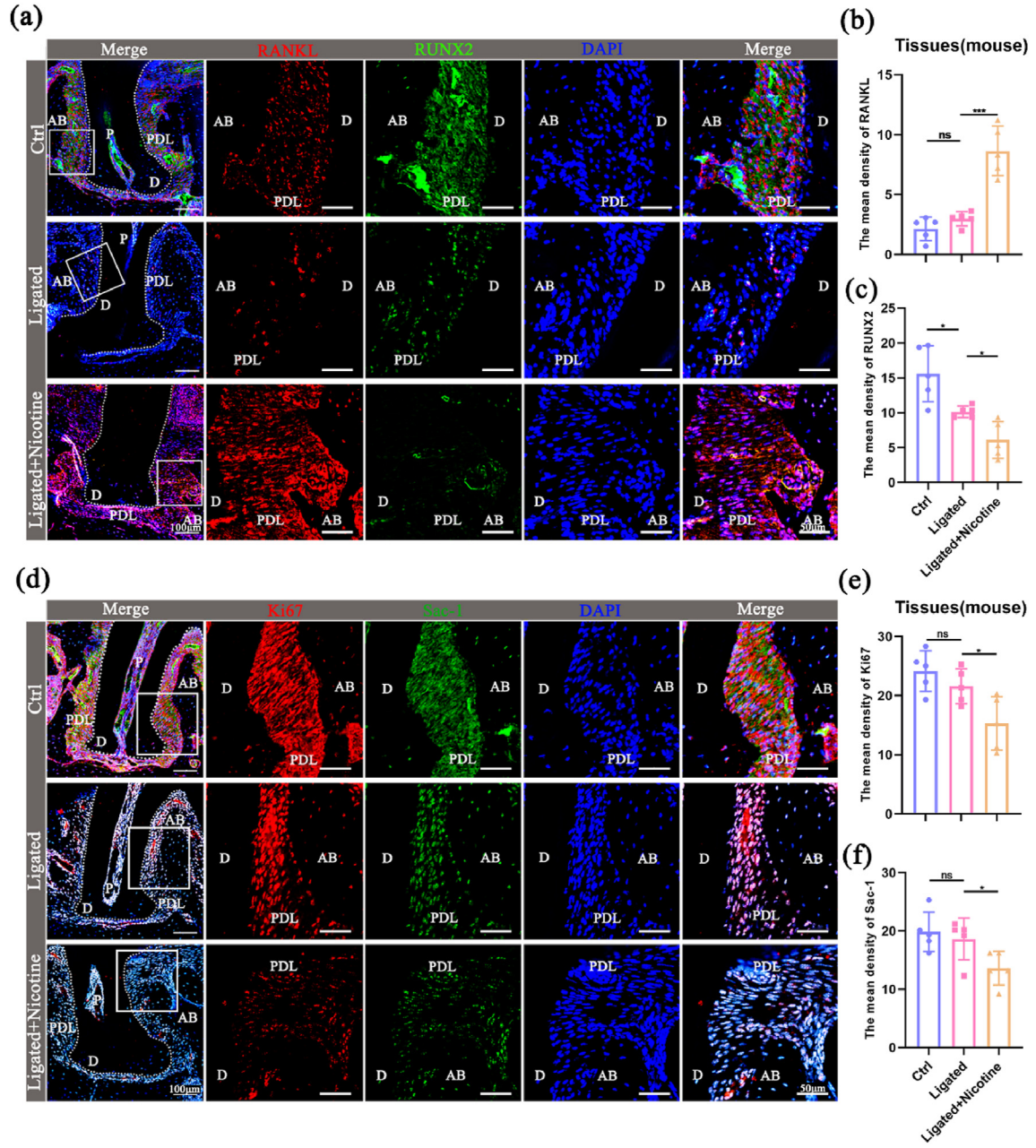

Figure 6 Nicotine affects the regenerative capability of endogenous dental stem cells in the periodontal ligament tissues of periodontitis mouse model. (a–c) Representative IF staining image reveals the increase of RANKL (red) expression and decrease of RUNX2 (green) expression in ligated + nicotine group versus ligated mice. (d–f) Representative IF staining image for proliferative markers in periodontal ligament. $Ki67^+$ and Sac-1+ cells are showed to decrease in periodontitis mice, and the nicotine treatment further inhibited the expression of Ki67 and Sac-1 in periodontal ligament tissues comparing with periodontitis mice. Ki67(red), Sac-1 (green), and DAPI (blue). D, dentine; PDL, periodontal ligament; AB, alveolar bone. Mean ± SD. ns $P > 0.05$. *$P < 0.05$. ***$P < 0.001$.

measured by the distance from the cementoenamel junction to the alveolar bone crest. (d) Masson staining to determine the fiber area in periodontal ligament of healthy, li-gated, and nicotine treated periodontitis mouse models. (e) Trap staining indicates the increasing densities of $TRAP^+$ osteoclastic-like cells (stained red) spreading around periodontal ligament in ligated + nicotine group comparing with ligated and control groups, which were indicated by black arrows. (f) Immunohitochemistry (IHC) shows increased area for inflammatory factors IL-1β, TNF-α, and IL-6 in ligated + nicotine group versus periodontitis and control groups. (g–k) Measurement of bone resorption in control, ligated, and nicotine + ligated groups. The nicotine + ligated group showed a greater bone resorption compared to ligated and control groups as measured by (g) bone volume/total volume (BV/TV), (h) trabecular separation (Tb.Sp), (i) trabecular number (Tb.N), (j) trabecular bone pattern factor (Tb.Pf), and (k) trabecular thickness (Tb.Th). Mean ± SD. ns $P > 0.05$. *$P < 0.05$. **$P < 0.01$. ***$P < 0.001$.

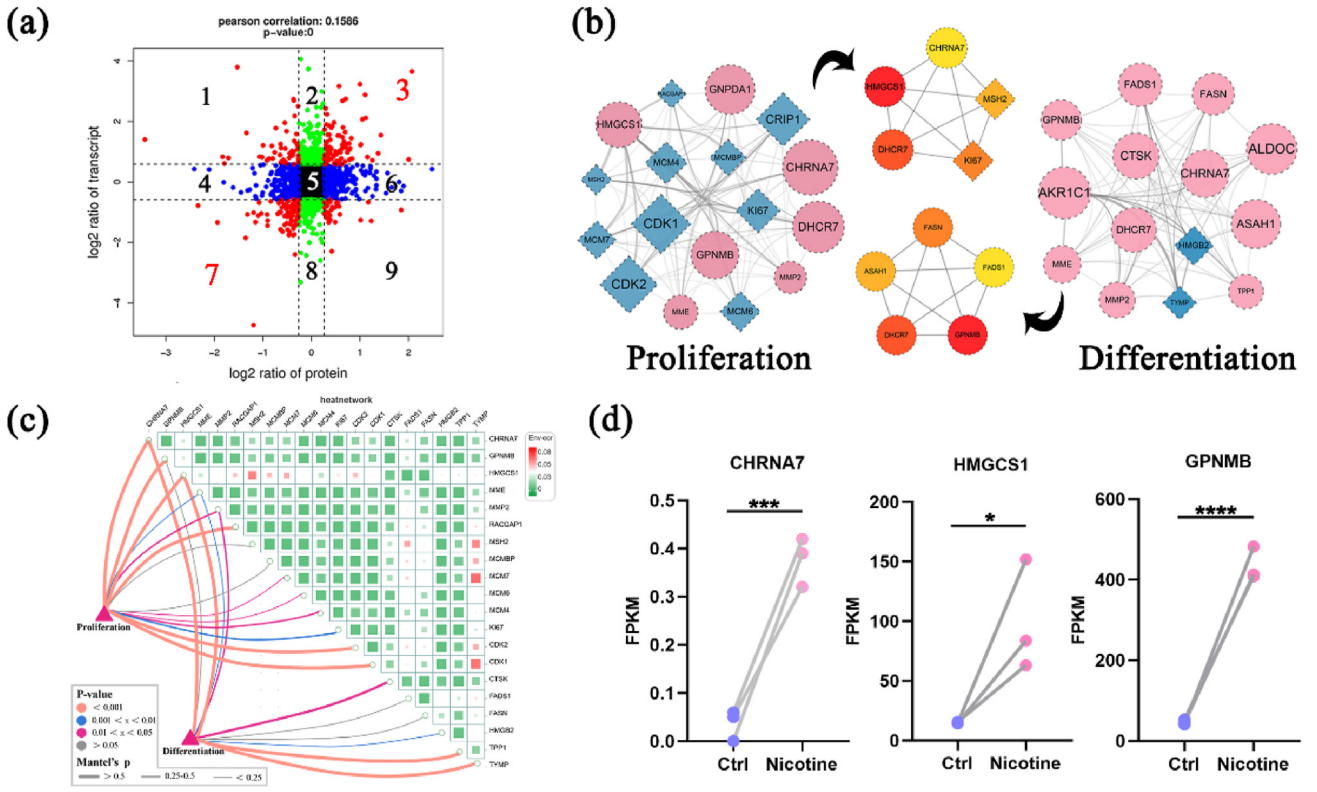

Figure 7 Key genes regulating regeneration in nicotine-treated hPDLSCs from multi-omics analysis of transcriptome and proteome. (a) A nine-quadrant volcano map reveals the elaborate expression changes of genes in transcriptome and proteome. The fifth quadrant shows genes with no significant different expressions both in mRNA and protein levels. The third and seven quadrants show genes that have same expression pattern in mRNA and protein levels. The first, second, and fourth quadrants show different expressed genes with lower protein expression changes versus mRNA expression changes. The sixth, eighth, and ninth quadrants show different expressed genes with higher protein expression changes versus mRNA expression changes. (b) PPI Networks of DEGs, performed by Cytoscape software. Genes correlated with proliferation (left) and differentiation (right) are both from the third and seventh quadrants. Red circle represents up-regulated genes and blue diamond represents down-regulated genes. Nodes size is positively associated with connectivity degree. Hub genes of proliferation and differentiation were screened by maximal clique centrality (MCC) algorithm from cytoHubba. Color gradient reveals different MCC scores. (c) Network diagram of the correlations between hPDLSCs regeneration phenotypes (proliferation and differentiation) and top 20 different expressed genes from the third and seventh quadrants. (d) FPKM values from RNA-seq showed that HMGCS1, GPNMB, and CHRNA7 were up-regulated treated by nicotine.

genetic variants[29–31] but limited to reflect protein dynamics because of post-transcriptional events.[32,33] Here, we performed the multi-omics integrative analysis of both transcriptomics and proteomics, which is one of the most promising approaches to the systemic investigation of stem cell biology, to provide bioinformatic evidence for the effect of nicotine on phenotypic alterations of hPDLSCs.[34] Owing to strong post-transcriptional regulation, the two data were not expected to overlap too much.[32,34] Besides, since the enrichment of small-size transcripts has not been done in this study, the transcriptomic analysis showed few information of miRNA in hPDLSCs after treatment of nicotine, which may be the other important reason that lead to the gap between transcriptomic and proteomic. To focus on cell regeneration-related genes that simultaneously escape post-transcriptional regulation, we classified differentially expressed genes into nine quadrants and selected three key genes. Taken together, our multi-omics analysis provided us key genes that potentially play crucial roles in the regeneration of nicotine-treated hPDLSC and may serve as novel biomarkers and targets for cellular therapy in smoking-related periodontitis.

The limitations of our study lie in that we discussed the effect of only nicotine on hPDLSCs and periodontitis animal models. In fact, tobacco smoke is a complex mixture containing more than 5000 chemicals,[35] although nicotine is the major substance in it. Hence, nicotine alone is insufficient to simulate the total smoking environment. Besides, since our multi-omics analysis provides large amounts of data, we only focused on the genes with same expression patterns in the two data sets while paying little attention to posttranscriptional modification of mRNAs. However, biochemical processes partially rely on post-transcriptional RNA modification. Therefore, it is also necessary to identify the RNA-modification sites for a better understanding of RNA-mediated biological functions and mechanisms.[36]

In conclusion, our study shows that nicotine exacerbates periodontitis by destructing periodontal tissue regeneration

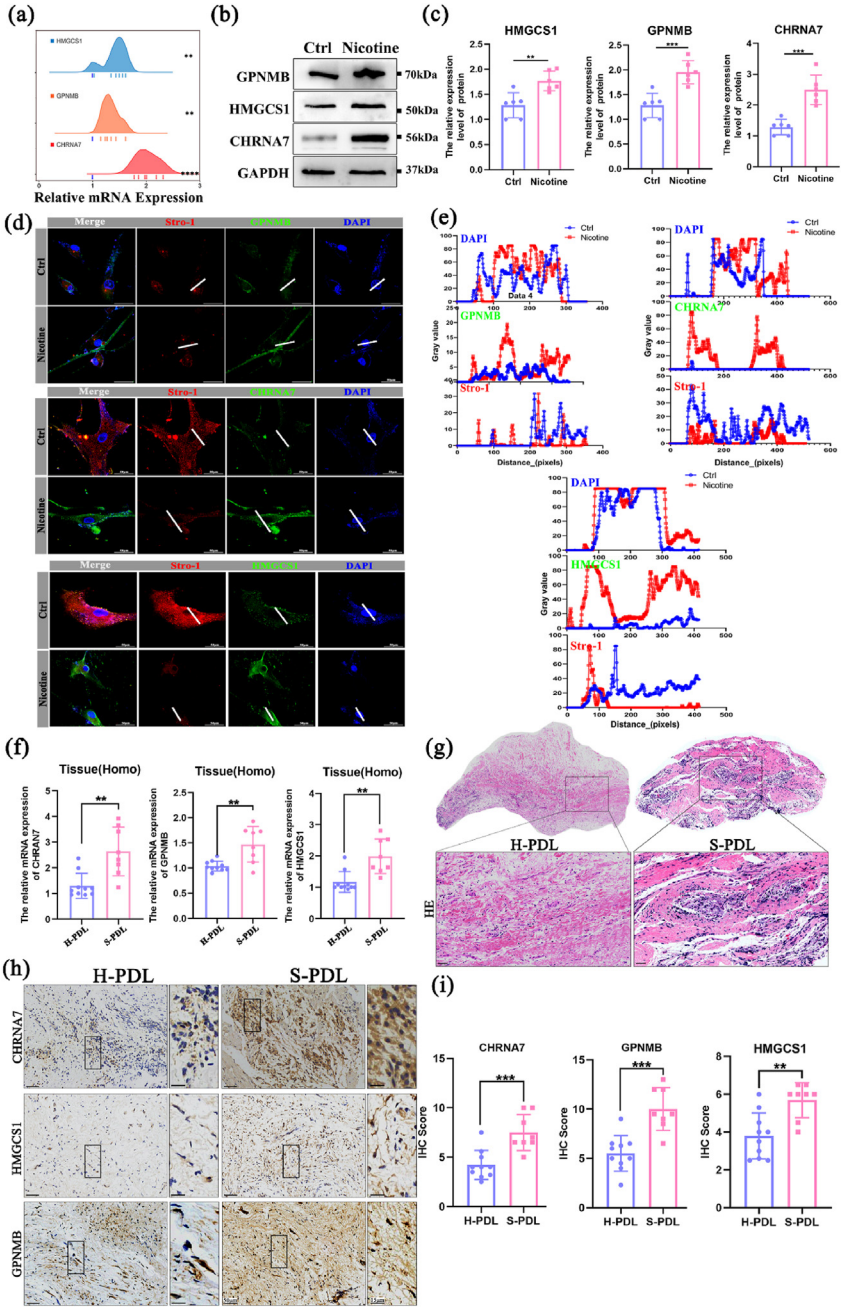

Figure 8 Confirmation for the expression of HMGCS1, GPNMB, and CHRNA7 in nicotine-treated hPDLSCs and human periodontal tissues influenced by smoking. (a–e) Validation for the expression of HMGCS1, GPNMB, and CHRNA7 in hPDLSCs. (a) Map of mountains shows the mRNA expressions of HMGCS1, GPNMB, and CHRNA7 from control and nicotine-treated hPDLSCs. The purple lines in the middle of the diagram represent the standard expression in control group, and different colored "mountains" represent the expressions of different genes in nicotine-treated group. (b, c) WB analysis to investigate the protein expression of HMGCS1, GPNMB, and CHRNA7 in control and nicotine-treated groups of hPDLSCs. GAPDH was used to control protein loading. Histogram on the right showed the quantification of the relative protein expression. (d) IF staining of Stro-1 with three key genes separately in control and nicotine-treated hPDLSCs. (e) The expression of Stro-1 and key genes were quantified by gray vales. The blue line represents the control group while the red line represents the nicotine-treated hPDLSCs. The horizontal axis represents specific distance of the targeted cells in each group. The results showed that the gray values of HMGCS1, GPNMB, and CHRNA7 in nicotine treated hPDLSCs (red line) were higher than control group (blue line). (f–i) Validation of HMGCS1, GPNMB, and CHRNA7 from human smoking and non-smoking periodontal ligament tissues. (f) qRT-PCR analysis of HMGCS1, GPNMB, and CHRNA7 from the human ligament periodontal tissues of 10 healthy donors and eight smokers. GAPDH was used for normalization relative to the control group. (g–i) Representative images of HE and IHC staining combined with IHC scores for HMGCS1, GPNMB, and CHRNA7 from different periodontal ligament tissues. H-PDL, healthy periodontal ligament; S-PDL, smoking-related periodontal ligament. Mean ± SD. $^{**}P < 0.01$. $^{***}P < 0.001$. $^{****}P < 0.0001$.

and impairing bone remodeling through inhibiting the proliferation and differentiation capabilities. The possible mechanisms include cell cycle arrest and imbalance of osteoblastogenesis/osteoclastogenesis in PDLSCs. HMGCS1, GPNMB, and CHRNA7 were characterized three key genes according to multi-omics analysis. In fact, CHRNA7 is one of the most important subunits among all functional nicotinic acetylcholine receptors (nAChRs), which plays a key role in nicotine exerting biological effects. Our previous study demonstrated that nicotine could regulate periodontal proinflammatory microenvironment by activating Wnt pathway through CHRNA7.[39] Besides, some research also suggested that nicotine could activate CHRNA7/JAK2/STAT3/SOX2 axis to improve the properties of esophageal squamous cell carcinoma (ESCC) and cancer-initiating cells (CIC).[40] However, the periodontal tissue regeneration effects of CHRNA7 in hPDLSCs under the treatment of nicotine still needs further investigation.

This study provides novel insights of modified personalized treatment targets for smoking patients and promotes contraindication in patients undergoing guided tissue regeneration based on dental stem cell therapy. In future studies, we will verify the role and mechanisms of key genes involved in smoking-related periodontitis and explore therapeutics for these patients.

Declaration of competing interest

All authors have no conflicts of interest relevant to this article.

Acknowledgments

This work was supported by grants from the National Natural Science Foundation of China (No. 81670988) and the National Clinical Medical Research Center for Oral Diseases of China (No. LCA202010).

Appendix A. Supplementary data

Supplementary data to this article can be found online at https://doi.org/10.1016/j.jds.2023.04.018.

References

1. Pihlstrom BL, Michalowicz BS, Johnson NW. Periodontal diseases. *Lancet* 2005;366:1809—20.
2. Kassebaum NJ, Bernabe E, Dahiya M, Bhandari B, Murray CJ, Marcenes W. Global burden of severe periodontitis in 1990—2010: a systematic review and meta-regression. *J Dent Res* 2014;93:1045—53.
3. Chaffee BW, Lauten K, Sharma E, et al. Oral health in the population assessment of tobacco and health study. *J Dent Res* 2022;101:1046—54.
4. Organization WH. *WHO monograph on tobacco cessation and oral health integration*. World Health Organization, 2017.
5. Nguyen B, Alpagot T, Oh H, Ojcius D, Xiao N. Comparison of the effect of cigarette smoke on mesenchymal stem cells and dental stem cells. *Physiol Cell Physiol* 2021;320:C175—81.
6. Johannsen A, Susin C, Gustafsson A. Smoking and inflammation: evidence for a synergistic role in chronic disease. *Periodontology* 2000 2014;64:111—26.
7. Samet JM, Wipfli HL. Globe still in grip of addiction. *Nature* 2010;463:1020—1.
8. Chen FM, Shelton RM, Jin Y, Chapple IL. Localized delivery of growth factors for periodontal tissue regeneration: role, strategies, and perspectives. *Med Res Rev* 2009;29:472—513.
9. Lin NH, Gronthos S, Bartold PM. Stem cells and future periodontal regeneration. *Periodontology* 2009;51:239—51.
10. Hyun SY, Lee JH, Kang KJ, Jang YJ. Effect of FGF-2, TGF-β-1, and BMPs on teno/ligamentogenesis and osteo/cementogenesis of human periodontal ligament stem cells. *Mol Cell* 2017;40:550—7.
11. Liu J, Chen B, Bao J, Zhang Y, Lei L, Yan F. Macrophage polarization in periodontal ligament stem cells enhanced periodontal regeneration. *Stem Cell Res Ther* 2019;10:320.
12. Queiroz A, Albuquerque-Souza E, Gasparoni LM, et al. Therapeutic potential of periodontal ligament stem cells. *World J Stem Cell* 2021;13:605—18.
13. Calabrese EJ. Human periodontal ligament stem cells and hormesis: enhancing cell renewal and cell differentiation. *Pharmacol Res* 2021;173:105914.
14. Mishra A, Chaturvedi P, Datta S, Sinukumar S, Joshi P, Garg A. Harmful effects of nicotine. *Indian J Med Paediatr Oncol* 2015;36:24—31.
15. Lindell G, Lunell E, Graffner H. Transdermally administered nicotine accumulates in gastric juice. *Eur J Clin Pharmacol* 1996;51:315—8.
16. Greenberg JM, Carballosa CM, Cheung HS. Concise review: the deleterious effects of cigarette smoking and nicotine usage and mesenchymal stem cell function and implications for cell-based therapies. *Stem Cells Transl Med* 2017;6:1815—21.
17. Lee J, Taneja V, Vassallo R. Cigarette smoking and inflammation: cellular and molecular mechanisms. *J Dent Res* 2012;91:142—9.
18. Nociti Jr FH, Casati MZ, Duarte PM. Current perspective of the impact of smoking on the progression and treatment of periodontitis. *Periodontology* 2015;67:187—210.
19. Fowler CD, Turner JR, Imad Damaj M. Molecular mechanisms associated with nicotine pharmacology and dependence. *Handb Exp Pharmacol* 2020;258:373—93.
20. Kang SK, Park YD, Kang SI, et al. Role of resistin in the inflammatory response induced by nicotine plus lipopolysaccharide in human periodontal ligament cells in vitro. *J Periodontal Res* 2015;50:602—13.
21. Song L, Li J, Yuan X, et al. Carbon monoxide-releasing molecule suppresses inflammatory and osteoclastogenic cytokines in nicotine- and lipopolysaccharide-stimulated human periodontal ligament cells via the heme oxygenase-1 pathway. *Int J Mol Med* 2017;40:1591—601.
22. Chaffee BW, Couch ET, Vora MV, Holliday RS. Oral and periodontal implications of tobacco and nicotine products. *Periodontology* 2021;87:241—53.
23. Zhang W, Lin H, Zou M, et al. Nicotine in inflammatory diseases: anti-inflammatory and pro-inflammatory effects. *Front Immunol* 2022;13:826889.
24. Schaal CM, Bora-Singhal N, Kumar DM, Chellappan SP. Regulation of Sox2 and stemness by nicotine and electronic-cigarettes in non-small cell lung cancer. *Mol Cancer* 2018;17:149.
25. Li Y, Wang M, Yang M, et al. Nicotine-induced ILF2 facilitates nuclear mRNA export of pluripotency factors to promote stemness and chemoresistance in human esophageal cancer. *Cancer Res* 2021;81:3525—38.
26. Solek P, Shemedyuk N, Shemedyuk A, Dudzinska E, Koziorowski M. Risk of wild fungi treatment failure: phallus impudicus-induced

telomere damage triggers p21/p53 and p16-dependent cell cycle arrest and may contribute to male fertility reduction in vitro. *Ecotoxicol Environ Saf* 2021;209:111782.
27. Qin Y, Liu Y, Jiang Y, et al. Cigarette smoke exposure inhibits osteoclast apoptosis via the mtROS pathway. *J Dent Res* 2021; 100:1378—86.
28. Zhou Z, Liu F, Wang L, et al. Inflammation has synergistic effect with nicotine in periodontitis by up-regulating the expression of α7 nAChR via phosphorylated GSK-3β. *J Cell Mol Med* 2020;24:2663—76.
29. Love MI, Huber W, Anders S. Moderated estimation of fold change and dispersion for RNA-seq data with DESeq2. *Genome Biol* 2014;15:550.
30. Pertea M, Kim D, Pertea GM, Leek JT, Salzberg SL. Transcript-level expression analysis of RNA-seq experiments with HISAT, StringTie and Ballgown. *Nat Protoc* 2016;11:1650—67.
31. Pertea M, Pertea GM, Antonescu CM, Chang TC, Mendell JT, Salzberg SL. StringTie enables improved reconstruction of a transcriptome from RNA-seq reads. *Nat Biotechnol* 2015;33: 290—5.
32. Chen Z, Zhao P, Li F, et al. Comprehensive review and assessment of computational methods for predicting RNA post-transcriptional modification sites from RNA sequences. *Briefings Bioinf* 2020;21:1676—96.
33. Schlieben LD, Prokisch H, Yépez VA. How machine learning and statistical models advance molecular diagnostics of rare disorders via analysis of RNA sequencing data. *Front Mol Biosci* 2021;8:647277.
34. Marchesan J, Girnary MS, Jing L, et al. An experimental murine model to study periodontitis. *Nat Protoc* 2018;13: 2247—67.
35. Talhout R, Schulz T, Florek E, van Benthem J, Wester P, Opperhuizen A. Hazardous compounds in tobacco smoke. *Int J Environ Res Publ Health* 2011;8:613—28.
36. Wörheide MA, Krumsiek J, Kastenmüller G, Arnold M. Multi-omics integration in biomedical research - a metabolomics-centric review. *Anal Chim Acta* 2021;1141:144—62.
37. Subramanian A, Tamayo P, Mootha VK, et al. Gene set enrichment analysis: a knowledge-based approach for interpreting genome-wide expression profiles. *Proc Natl Acad Sci USA* 2005;102:15545—50.
38. Zhou Y, Zhou B, Pache L, et al. Metascape provides a biologist-oriented resource for the analysis of systems-level datasets. *Nat Commun* 2019;10:1523.
39. Zhou Z, Li B, Dong Z, et al. Nicotine deteriorates the osteogenic differentiation of periodontal ligament stem cells through α7 nicotinic acetylcholine receptor regulating Wnt pathway. *PLoS One* 2013;8:e83102.
40. Wang L, Du L, Xiong X, et al. Repurposing dextromethorphan and metformin for treating nicotine-induced cancer by directly targeting CHRNA7 to inhibit JAK2/STAT3/SOX2 signaling. *Oncogene* 2021;40:1974—87.